Two-oscillator model of ventilatory rhythmogenesis in the frog

Amitabha Bose, [a],* Timothy J. Lewis, [b]
and Richard J. A. Wilson [c] [1]

[a] *Dept. Mathematical Sciences, New Jersey Institute of Technology, Newark, NJ*

[b] *Department of Mathematics, University of California, Davis, CA*

[c] *Dept. Medical Physiology and Biophysics, University of Calgary, Calgary, Alberta, Canada.*

Abstract

Frogs produce two distinct yet highly coordinated ventilatory behaviors, buccal and lung. Lung ventilation occurs in short episodes, interspersed with periods of buccal ventilation. Recent data suggests that two brainstem oscillators are involved in generating these behaviours, one primarily responsible for buccal ventilation, the other for lung. Here we use a modeling approach to demonstrate that the episodic pattern of lung ventilation might be an emergent property of the coupling between the oscillators, and may not require a perturbing input from another, as yet unidentified but previously postulated, neuronal oscillator.

Key words: Coupled oscillators, brainstem, respiration, ventilation, synaptic facilitation, respiratory rhythm

1 Introduction

Breathing is a complicated multiphasic motor act, involving the precise coordination of a large number of muscles. Recent studies in chicks (1), embryonic mice (2) and neonatal rats (3) using isolated brainstem preparations suggest that developing respiratory rhythm generators consist of at least two brainstem sites that have independent rhythmogenic capability. In the frog, coupled

---

[1] All authors contributed equally to this work.

* Corresponding author.
  Email address: `bose@njit.edu` (Amitabha Bose,).

respiratory oscillators have been identified in the brainstem of juvenile animals (4), suggesting that the use of multiple oscillators in respiratory rhythm generation may extend beyond development. Understanding how these 'neuronal oscillators' communicate and coordinate their activity is poorly understood and represents a major challenge for respiratory neuroscience.

In the frog, there are two distinct, but highly coordinated forms of ventilation, tidal ventilation of the buccal cavity (buccal ventilation) and tidal ventilation of the lungs (lung ventilation). The distinct motor patterns corresponding to these two forms of ventilation, known as buccal and lung bursts, are produced by cranial and spinal nerves and are observable in an isolated brainstem preparation (5; 6). When the partial pressure of carbon dioxide (PCO_2) of the saline used to perfuse the preparation is low, activity is dominated by small amplitude buccal bursts (the default mode), but as PCO_2 is elevated, buccal bursts are replaced progressively by clusters of large amplitude lung bursts (7).

Recently, Wilson *et al* (4) identified two loci within the brainstem that are important for the generation of these motor patterns: a rostral site necessary and sufficient for lung bursts, and a caudal site necessary and sufficient for buccal bursts. When the brainstem was transected between these sites, the caudal half produced continuous buccal-like bursts, whereas the rostral half produced occasional large amplitude bursts. Based on these data and the results of several pharmacological studies, Wilson *et al* (4) proposed a coupled oscillator model for the respiratory rhythm generator in the frog (see Figure 1). This schematic model helps to explains how lung and buccal ventilation is coordinated, but does not explicitly address the switching back and forth between buccal and lung episodes.

It has been postulated that an external, as yet unidentified, neuronal oscillator is needed to control the switching between the buccal and lung episodes. Our model suggests that a third oscillator may not be necessary. Here, we study an idealized computational model of two coupled oscillators and we show that the switching between motor patterns (buccal and lung episodes) may be an
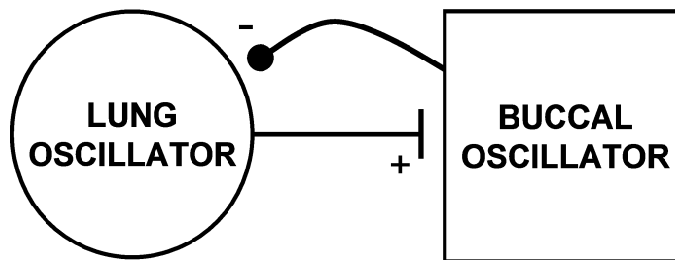

Fig. 1. A schematic diagram of the proposed neuronal circuit. The circuit is composed of a lung oscillator (L) and buccal oscillator (B). When L is active, it excites B; when B is active, it inhibits L. The B to L inhibitory connection is hypothesized to be a facilitating synapse.

emergent property of a two coupled oscillator network.

2   Model and Methods

The minimal model consists of one lung (L) and one buccal (B) oscillator, where each oscillator is likely to represent the activity of a population of neurons. There is an excitatory synapse from the lung to the buccal oscillator, and a facilitating inhibitory synapse from the buccal to the lung oscillator. We have constructed the model to be consistent with the experimental observations in Wilson et al (4). We use a canonical neuronal model (the Morris-Lecar equations (8)) to describe the burst envelope of each of the oscillators. These equations, together with those describing dynamics of the synapses between oscillators, are:

$$c\,v'_L = I_{app,L} - I_{leak}(v_L) - I_K(v_L, w_L) - I_{Ca}(v_L) - g_{inh}s_B[v_L - E_{inh}] \quad (1)$$
$$w'_L = \psi\lambda(v_L)[w_\infty(v_L) - w_L] \quad (2)$$
$$c\,v'_B = I_{app,B} - I_{leak}(v_B) - I_K(v_B, w_B) - I_{Ca}(v_B) - g_{exc}s_L[v_B - E_{exc}] \quad (3)$$
$$w'_B = \phi(v_B)\lambda(v_B)[w_\infty(v_B) - w_B] \quad (4)$$
$$s'_L = \nu[1 - s_L]s_\infty(v_L) - \eta s_L[1 - s_\infty(v_L)] \quad (5)$$
$$s'_B = \gamma[d_B - s_B]s_\infty(v_B) - \kappa s_B[1 - s_\infty(v_B)] \quad (6)$$
$$d'_B = [1 - d_B]d_\infty(v_B)/\tau_\alpha - d_B[1 - d_\infty(v_B)]/\tau_\beta \quad (7)$$

where v_L and v_B denote the voltage of the lung and buccal oscillators, and w_L and w_B are the potassium based recovery variables, respectively. The ionic currents in Eq.1 and Eq.3 are given by $I_{leak}(v) = g_l[v - E_l]$, $I_K(v, w) = g_K w[v - E_K]$ and $I_{Ca}(v) = g_{Ca}m_\infty(v)[v - E_{Ca}]$, $m_\infty = 0.5[1 + \tanh(v - v_1)/v_2]$. The functions $w_\infty(v) = 0.5[1 + \tanh(v - v_3)/v_4]$, $\lambda(v) = [\cosh(v - v_3)/2v_4]$, $d_\infty(v) = 0.5[1 + \tanh(v - v_5)/v_6]$, $s_\infty = 0.5[1 + \tanh(v - v_7)/v_8]$ and $\phi(v_B) = [\phi_L + [\phi_R - \phi_L]][0.5[1 + \tanh(v_B - v_9)/v_{10}]$. Parameter values are $c = 20$, $\psi = 0.04$, $\phi_R = 0.009$, $\phi_L = 0.1$, $v_1 = -1.2$, $v_2 = 18$, $v_3 = 11$, $v_4 = 30$, $v_5 = -15$, $v_6 = 0.01$, $v_7 = 0$, $v_8 = 18$, $v_9 = 0$, $v_{10} = 0.01$, $g_l = 2$, $g_{Ca} = 4.4$, $g_K = 8$, $E_l = -60$, $E_{Ca} = 120$, $E_K = -84$. The applied current $I_{app} = 96$ for L and 110 for B. Note that v_5 is the threshold for facilitation of the inhibitory synapse and v_7 is the threshold of synaptic transmission. Note further that all variables and parameters are in dimensionless units.

The synapse from L to B is excitatory and is governed by Eq.5. The parameters $g_{exc} = 5$, $E_{exc} = 0$, $\nu = 1$, $\eta = 1$ indicating that this a strong and fast synapse. The synapse from B to L is inhibitory and facilitating. The strength of a facilitating synapse increases as a function of usage. The equations used to describe its dynamics are given in Eq.6-7 and are based on a model of short-term synaptic plasticity used in (9). The variable d_B measures the level

of facilitation of the synapse, while s_B incorporates this information to L in Eq.1. Specifically when $v_B > v_5$, the synapse facilitates and d_B increases towards one with time constant $\tau_\alpha = 1250$. When $v_B < v_5$, the synapse de-facilitates and it decreases towards zero with time constant $\tau_\beta = 22$. The variable s_B is coupled to d_B when $v_B > v_7(= 0)$. Then s_B increases towards d_B with rate $\gamma = 1$. Note that this rate is relatively large implying that s_B is effectively equal to d_B whenever $V_B > 0$. When $V_B < 0$, s_B is decoupled from d_B and decays towards 0 with rate $\kappa = 0.5$, which is equivalent to a fast decay of inhibition. The parameters $g_{inh} = 0.4$ and $E_{inh} = -75$.

3 Results

The main purpose of our work is to show that a two oscillator model can automatically produce the switching between lung- and buccal-driven episodes of breathing. We first show simulation results that illustrate the two different forms of ventilation and the switching between them. We then describe the basic mechanisms behind this phenomena using concepts from bifurcation theory.

In Figure 2, we show simulation results from our network. The equations were solved using the software XPP (10). The rhythmic pattern switches between lung- and buccal-driven episodes as indicated in the figure. For the parameters chosen, there happens to be two buccal oscillations for every four lung oscillations. During the lung-driven episode, both L and B are actively bursting ('on'). The facilitation variable d_B increases monotonically because v_B is always greater than the threshold for facilitation, v_5. This causes the inhibition to L to increase with each burst of L and B as the variable s_B attains the value of d_B whenever v_B increases through zero. Eventually, the inhibition becomes strong enough to completely suppress lung oscillations, and the rhythm switches to the buccal-driven mode.

During the buccal-driven episode, the strongly inhibited L is not active ('off'), and B undergoes its intrinsic oscillatory dynamics. During part of the bursting cycle, v_B falls below v_5. Because the time constant τ_β is not too large, this causes a fairly rapid de-facilitation of the synapse (i.e. a decrease in the level of facilitation). However, v_B spends relatively little time below v_5. Thus, it takes two buccal oscillations before inhibition from B to L is weakened by the synaptic de-facilitation to the point that allows L to fire. In other words, the inhibition from B becomes too weak to continue to suppress L firing.

Next we will explain why the system switches between these two oscillatory modes and does not remain fixed in a single mode of ventilation. Let us first consider the lung oscillator under fixed levels of inhibition. With no inhibitory
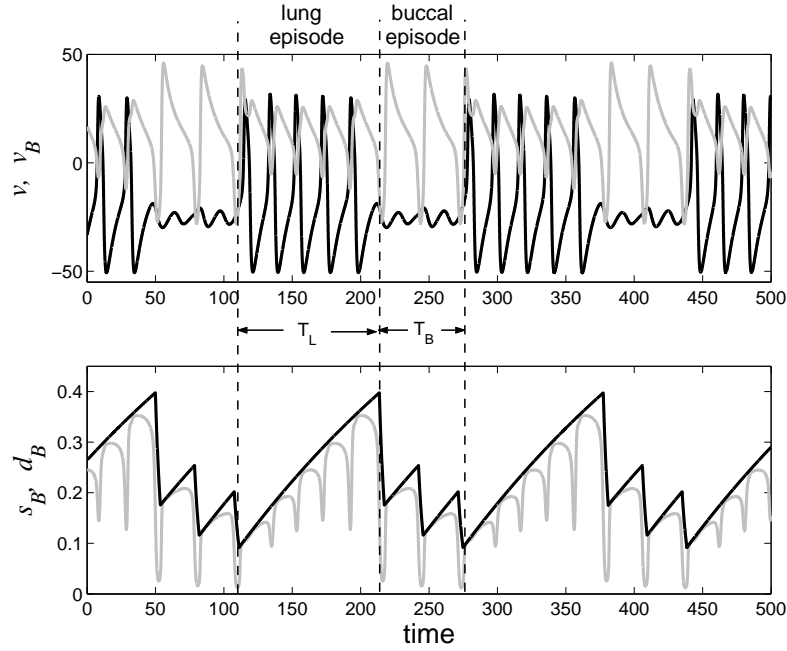
4

Fig. 2. An example of oscillations in which there is switch between two different types of rhythms: lung and buccal. **[top]** v_L (black) and v_B (gray) versus time; lung and buccal episodes are indicated. **[bottom]** s_B (gray) and d_B (black) versus time.

input, the lung oscillator undergoes stable large amplitude oscillations. At sufficiently high levels of inhibition, the inhibitory input kills off the oscillations and only a quiescent state exists. However, in an intermediate range of inhibition, both of these behaviors co-exist (i.e. bistability exists). That is, as the level of inhibition changes, the system undergoes a subcritical Hopf bifurcation and the large amplitude oscillation arise/disappear via a limit point bifurcation. The bifurcation diagram is plotted in Figure 3.

Now let us consider the full system and how the lung and buccal oscillators affect one another. Assume that the system is initially at the beginning of a buccal episode. At this time, because there is no input onto the buccal oscillator, the buccal undergoes its intrinsic oscillations. Furthermore, inhibition on the lung oscillator from the buccal oscillator is very high and the lung is quiescent. That is, the system is effectively on the stable quiescent branch of the lung bifurcation diagram at point A. The intrinsic buccal oscillations have a relatively short duty cycle and therefore a relatively low level of buccal firing. This causes the buccal to lung inhibitory synapse to slowly de-facilitate and the inhibition of the lung oscillator slowly weakens (the net inhibition s_B decreases). Thus, the system move from point A to point B along the stable quiescent branch of the lung bifurcation diagram.

Eventually inhibition becomes so weak that the system reaches point B and the quiescent state of the lung oscillator loses stability. The lung oscillator then begins to fire in an oscillatory manner. That is, the system has moved
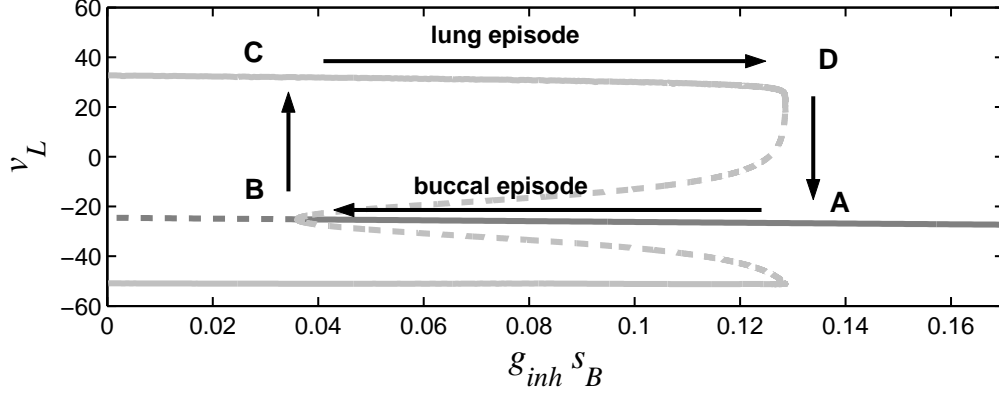
Fig. 3. The bifurcation diagram of the lung oscillator L in response to constant inhibition $g_{inh}s_B$: Dark gray lines represent the value of v_L at steady state solutions (quiescent states); light gray represent minimum and maximum values of v_L on periodic orbits (oscillating states). Solid and dashed curves signify stable and unstable solutions, respectively. The dynamics of synaptic facilitation lead to hystersis between the quiescent and oscillating states as indicated by the arrows on the branches of bifurcation diagram.

through the subcritical Hopf bifurcation and has moved to point C on the periodic solutions branch of the lung bifurcation diagram. Thus, there is a switch from the buccal to lung episode. The activity of the lung oscillator increases the excitatory drive to the buccal and, in doing so, increases the duty cycle of the buccal. This in turn causes the inhibitory synapse to begin to slowly facilitate and the system moves from point C towards point D, along the branch of periodic solutions on the lung bifurcation diagram.

Eventually the buccal-to-lung inhibitory synapse facilitates so much that the system reaches point D on the bifurcation diagram. Here, inhbition shuts down the oscillatory activity in the lung oscillator via the limit point bifurcation. The system then returns to point A on the lung bifurcation diagram (i.e. the initial point of the buccal episode), and the pattern begins again.

In Figure 2, it is easy to note that d_B oscillates between a maximum and minimum value, d_{max} and d_{min}. The values d_{max} and d_{min} can be calculated by finding the values at which the system of equations undergoes a limit point bifurcation of periodic orbits (points A & D) and a subcritical Hopf bifurcation (points B & C), respectively. Let T_L denote the time the network spends in a lung-driven episode and T_B the time spent in a buccal-driven episode. The time T_L is then the time it takes for d_B to increase from d_{min} to d_{max} and the time T_B is the time needed to decrease from d_{max} to d_{min}. Note that the increase of d_B is monotonic during a lung episode, wherease d_B both increases and decreases during a buccal episode. The duration of a lung-driven episode T_L and the number of lung bursts within an episode can be increased by making the facilitation time constant τ_α larger. Alternatively, by making the

time constant for de-facilitation τ_β larger, we can increase the duration T_B of the buccal-driven episode and the number of buccal bursts in an episode (simulations not shown).

4 Conclusions

This work is proof of principle that the switching back and forth between lung and buccal episodes may be an emergent property of the coupling between these oscillators. Consequently, external input regulating the switching between episodes may not be necessary.

In the context of our modeling framework, bistability and a slow time-dependent process are essential for episodes. In the current model, the bistabilty is intrinsic to the lung oscillator; the slow time-dependent process lies in the facilitation of the inhibitory synapse from the buccal to the lung oscillator. However, in the biological circuit, the bistability and the slow time-dependent process may reside elsewhere and could be distributed across multiple sites within the circuit.

References

[1] G. Fortin, P. Charnay, J. Champagnat, Linking respiratory rhythm generation to segmentation of the vertebrate hindbrain, Pflugers Arch. 446 (2003) 514–515.

[2] V. Abadie, J. Champagnat, G. Fortin, Branchiomotor activities in mouse embryo, Neuroreport 11 (2000) 141–145.

[3] N. Mellen, W. Janczewski, C. Bocchiaro, J. Feldman, Opioid-induced quantal slowing reveals dual networks for respiratory rhythm generation, Neuron 37 (2003) 821–826.

[4] R. Wilson, K. Vasilakos, M. B. Harris, C. Straus, J. E. Remmers, Evidence that ventilatory rhythmogenesis in the frog involves two distinct neuronal oscillators, J. Physiol. 540 (2002) 557–570.

[5] N. Kogo, S. Perry, J. Remmers, Neural organization of the ventilatory activity in the frog, *rana catesbeiana*, Journal of Neurobiology 25 (1994) 1067–1069.

[6] M. J. Gdovin, C. Torgerson, J. Remmers, Neurorespiratory pattern of gill and lung ventilation in the decerebrate spontaneously breathing tadpole, Respiratory Physiology 113 (1998) 135–146.

[7] C. S. Torgerson, M. J. Gdovin, J. Remmers, Ontogeny of central chemoreception during fictive gill and lung ventilation in an in vitro brainstem preparation of rana catesbeiana, Journal of Experimental Biology 200 (1997) 2063–2972.

[8] C. Morris, H. Lecar, Voltage oscillations in barnacle giant muscle fiber, Biophys. J. 35 (1981) 193–213.

[9] A. Bose, Y. Manor, F. Nadim, Bistability arising from synaptic depression, SIAM J. App. Math 62 (2001) 706–727.

[10] B. Ermentrout, Simulation, Analyzing, and Animating Dynamical Systems: A Guide to XPPAUT for Researchers and Students, SIAM, Philadelphia, PA, 2002.